



Genome-Wide CRISPR-Cas9 Screen Reveals the Importance of the Heparan Sulfate Pathway and the Conserved Oligomeric Golgi Complex for Synthetic Double-Stranded RNA Uptake and Sindbis Virus Infection

Olivier Petitjean,^a  Erika Girardi,^a  Richard Patryk Ngondo,^b  Vladimir Lupashin,^c  Sébastien Pfeffer^a

^aUniversité de Strasbourg, Architecture et Réactivité de l'ARN, Institut de Biologie Moléculaire et Cellulaire du CNRS, Strasbourg, France

^bUniversité de Strasbourg, Institut de Biologie Moléculaire des Plantes du CNRS, Strasbourg, France

^cUniversity of Arkansas for Medical Sciences, Little Rock, Arkansas, USA

Olivier Petitjean and Erika Girardi contributed equally. Author order was determined on the basis of increasing seniority.

ABSTRACT Double-stranded RNA (dsRNA) is the hallmark of many viral infections. dsRNA is produced either by RNA viruses during replication or by DNA viruses upon convergent transcription. Synthetic dsRNA is also able to mimic viral-induced activation of innate immune response and cell death. In this study, we employed a genome-wide CRISPR-Cas9 loss-of-function screen based on cell survival in order to identify genes implicated in the host response to dsRNA. By challenging HCT116 human cells with either synthetic dsRNA or Sindbis virus (SINV), we identified the heparan sulfate (HS) pathway as a crucial factor for dsRNA entry, and we validated SINV dependency on HS. Interestingly, we uncovered a novel role for COG4, a component of the conserved oligomeric Golgi (COG) complex, as a factor involved in cell survival to both dsRNA and SINV in human cells. We showed that COG4 knockout led to a decrease of extracellular HS that specifically affected dsRNA transfection efficiency and reduced viral production, which explains the increased cell survival of these mutants.

IMPORTANCE When facing a viral infection, the organism has to put in place a number of defense mechanisms in order to clear the pathogen from the cell. At the early phase of this preparation for fighting against the invader, the innate immune response is triggered by the sensing of danger signals. Among those molecular cues, double-stranded RNA (dsRNA) is a very potent inducer of different reactions at the cellular level that can ultimately lead to cell death. Using a genome-wide screening approach, we set to identify genes involved in dsRNA entry, sensing, and apoptosis induction in human cells. This allowed us to determine that the heparan sulfate pathway and the conserved oligomeric Golgi complex are key determinants allowing entry of both dsRNA and viral nucleic acid leading to cell death.

KEYWORDS CRISPR-Cas9 screen, complex oligomeric Golgi complex, double-stranded RNA, heparan-sulfate, transfection, virus


Upon infection by a virus, numerous mechanisms are put in place at the cellular level to raise the alarm and get rid of, or at least limit, the invader. One of the first barriers that the virus has to overcome is cell entry, which is done by taking advantage of a wide diversity of ubiquitous or cell-specific cellular receptors. In addition to protein receptors, glycosaminoglycans present at the cell surface represent crucial factors for efficient viral attachment and entry (1). Glycosaminoglycans, and more precisely heparan sulfates (HSs), are ubiquitously expressed in human cells. They possess a global

Citation Petitjean O, Girardi E, Ngondo RP, Lupashin V, Pfeffer S. 2020. Genome-wide CRISPR-Cas9 screen reveals the importance of the heparan sulfate pathway and the conserved oligomeric Golgi complex for synthetic double-stranded RNA uptake and Sindbis virus infection. *mSphere* 5:e00914-20. <https://doi.org/10.1128/mSphere.00914-20>.

Editor Urs F. Greber, University of Zurich

Copyright © 2020 Petitjean et al. This is an open-access article distributed under the terms of the [Creative Commons Attribution 4.0 International license](https://creativecommons.org/licenses/by/4.0/).

Address correspondence to Sébastien Pfeffer, spfeffer@unistra.fr.

 Genome-Wide CRISPR-Cas9 Screen Reveals the Importance of the Heparan Sulfate Pathway and the Conserved Oligomeric Golgi Complex for Synthetic Double-Stranded RNA Uptake and Sindbis Virus Infection @LabPfeffer

Received 10 September 2020

Accepted 26 October 2020

Published 11 November 2020

negative charge that is able to interact electrostatically with the basic residues that are exposed by viral surface glycoproteins. This allows viruses to increase their concentration at the cell surface and thus the possibility to interact with their specific entry receptor (2). For instance, alphaviruses, such as Semliki Forest virus (SFV) and Sindbis virus (SINV), are enveloped positive-strand RNA viruses that contain two glycoproteins at the envelope, namely, the proteins E1 and E2. E2 is involved in the interaction of the virus particle with the cell surface (3, 4), while E1 serves in the fusion process (5).

Once the virus is inside the cell, the replication of the viral genome represents another critical step for triggering the antiviral immune response. Double-stranded RNA (dsRNA) is a ubiquitous pathogen-associated molecular pattern (PAMP) recognized by the cellular machinery, which can arise as a replication intermediate for viruses with an RNA genome or from convergent transcription for DNA viruses (6). In mammals, dsRNA recognition is driven by specific receptors, including the cytoplasmic RIG-like receptors (RLRs) and endosomal Toll-like receptors (TLRs) (7). Sensing of dsRNA by these receptors results in the activation of a complex signaling cascade leading to the production of type I interferon (IFN), which in turn triggers the expression of IFN-stimulated genes (ISGs) and the establishment of the antiviral state (8). The ultimate outcome of this vertebrate-specific antiviral response is translation arrest and cell death by apoptosis (9).

The revolution brought by the discovery of the CRISPR-Cas9 technology has provided biologists with an invaluable tool for editing the genome at will and easily performing individual gene knockout (KO) (10). This technique is perfectly suited to perform genome-wide screens in a relatively fast and easy-to-implement manner, especially when the readout is based on cell survival. For this reason, numerous CRISPR-Cas9 loss-of-function screens have been performed based on cell survival after infection with different viruses (11–13). These approaches allowed the identification of novel virus-specific as well as common factors involved in antiviral defense mechanisms or in cellular permissivity to virus infection.

Here, we chose to take advantage of the fact that dsRNA is almost always detected in virus-infected cells (6) and is a potent inducer of apoptosis to design a genome-wide screen aimed at identifying host genes that when edited resulted in increased cell survival to dsRNA and viral challenge. To this aim, we performed a CRISPR-Cas9 screen based on cell survival in HCT116 cells after either cationic lipid-based transfection of an *in vitro*-transcribed long dsRNA or infection with the model alphavirus SINV, which replicates via a dsRNA intermediate.

Our results indicate that genes involved in limiting attachment and therefore entry, be it of the synthetic dsRNA or SINV, are vastly overrepresented after selection. We validated two genes of the heparan sulfate pathway (namely, *SLC35B2* and *B4GAL7*) as being required for dsRNA transfectability and SINV infectivity. We also identified and characterized COG4, a component of the conserved oligomeric Golgi (COG) complex, as a novel factor involved in susceptibility to dsRNA and viral-induced cell death linked to the heparan sulfate biogenesis pathway.

RESULTS

Genome-wide CRISPR-Cas9 screen based on cell survival upon dsRNA transfection identifies factors of the heparan sulfate pathway. In order to identify cellular genes that are involved in the cellular response to dsRNA, which culminates with cell death, we performed a CRISPR-Cas9 genome-wide loss-of-function screen in the human colon carcinoma cell line HCT116. This cell line is highly suitable for CRISPR-Cas9 genetic screening procedures (14) and can be easily infected with SINV with visible cytopathic effects at 24 and 48 hours postinfection (hpi) (see Fig. S1A in the supplemental material). Moreover, transfection of an *in vitro*-transcribed 231-bp-long dsRNA by a cationic lipid-based transfection reagent in HCT116 cells led to strong cell death at 24 and 48 hours posttreatment (hpt) (Fig. S1B).

We generated a Cas9-expressing HCT116 monoclonal cell line (Fig. S1C) that we stably transduced with the human genome-wide lentiviral Brunello library composed of

76,441 single guide RNAs (sgRNAs) targeting 19,114 genes, as well as about 1,000 nontargeting sgRNAs as controls (15). We then applied a positive selection by lipofection of 30 million transduced cells per replicate with the synthetic long dsRNA, and we collected the surviving cells 48 h later. In parallel, the same initial amount of stably transduced cells was left untreated as a control (input) for each replicate (Fig. 1A). DNA libraries from the input samples were generated, sequenced, and quality checked. In particular, we verified the sgRNA coverage by observing the presence of the 4 guides per gene for 18,960 genes (99.2% of the genes) and 3 sgRNAs per gene for the remaining 154 genes (0.2% of the genes) (see Data Set S1 in the supplemental material).

Using the MAGeCK software (16), we assessed the normalized read count distribution of the control and dsRNA-treated biological triplicates, which, despite a quite homogenous sgRNA distribution, showed the presence of few outliers upon selection (Fig. 1B). We identified eight genes that were significantly enriched with a false discovery rate lower than 1% (FDR1%). Among those genes, four belonged to the heparan sulfate biosynthesis pathway (namely, *SLC35B2*, *B4GALT7*, *EXT1*, and *EXT2*) and three were components of the conserved oligomeric Golgi complex (namely, *COG3*, *COG4*, and *COG8*) (Fig. 1C; see Data Set S2 in the supplemental material). In particular, all four sgRNAs targeting each of the *SLC35B2*, *B4GALT7*, and *COG4* genes were enriched upon dsRNA selection (Fig. S1D).

Heparan sulfate is a linear polysaccharide that is covalently attached to core proteins in proteoglycans (PGs) on the cell surface (for review, see reference 17). Among many properties, HS plays a role in binding protein ligands and as a carrier for lipases, chemokines, and growth factors (17, 18), but also as a viral receptor (19). HS biosynthesis takes place in the Golgi, where most of the biosynthetic enzymes are anchored to the Golgi membrane (20).

We first validated the resistance phenotype to dsRNA of *SLC35B2* and *B4GALT7*, the two top hits identified in the screen (Fig. 1C, Fig. S1D), by generating two individual knockout clones for each gene by CRISPR-Cas9 editing in HCT116cas9 cells (see Fig. S2 in the supplemental material). Knockout of either *SLC35B2* or *B4GALT7* genes abolished cell death induced by dsRNA lipofection compared with parental HCT116cas9 cells, as assessed by the measurement of cell viability 48 h posttransfection (Fig. 1D, left part of the graph). These results demonstrated the involvement of *SLC35B2* and *B4GALT7* in dsRNA-induced cell death.

The observed resistance to dsRNA in the mutants could occur at many different steps, namely, dsRNA liposome attachment and entry, recognition, induction of the IFN pathway, or apoptosis. To test whether the first step was affected, we employed a nucleic acid delivery method that was not based on cationic lipid transfection. In particular, we used nucleofection (an electroporation-based transfection method) to introduce long dsRNAs into HCT116 cells, and we showed that this approach restored cell death in *SLC35B2* and *B4GALT7* knockout cells (Fig. 1D, right part of the graph). In addition, we performed liposome-based transfection of an *in vitro*-transcribed Cy5-labeled dsRNA in *SLC35B2* and *B4GALT7* KO cells and assessed the Cy5 fluorescence at 48 h posttransfection by fluorescence-activated cell sorter (FACS) analysis (Fig. 1E and F). Although the number of Cy5 positives (Cy5+) cells was not significantly different in the *B4GALT7* KO clones and was only slightly lower in the *SLC35B2* KO cells than in wild-type (WT) cells (Fig. 1E), we observed a significant reduction of at least 80% of the median Cy5 fluorescence in both *B4GALT7* and *SLC35B2* KO cells relative to the control (Fig. 1F), thereby indicating a significant drop in the number of transfected Cy5-labeled RNA molecules per cell.

We also confirmed that liposome-based transfection of nucleic acids, such as plasmidic DNA, was impaired in *SLC35B2* and *B4GALT7* KO cells by transfecting a green fluorescent protein (GFP)-expressing plasmid using Lipofectamine 2000 in wild-type or knockout cells (see Fig. S3A, left, and Fig. S3B in the supplemental material). Nonetheless, GFP expression could be restored in all cell lines upon nucleofection (Fig. S3A, right).

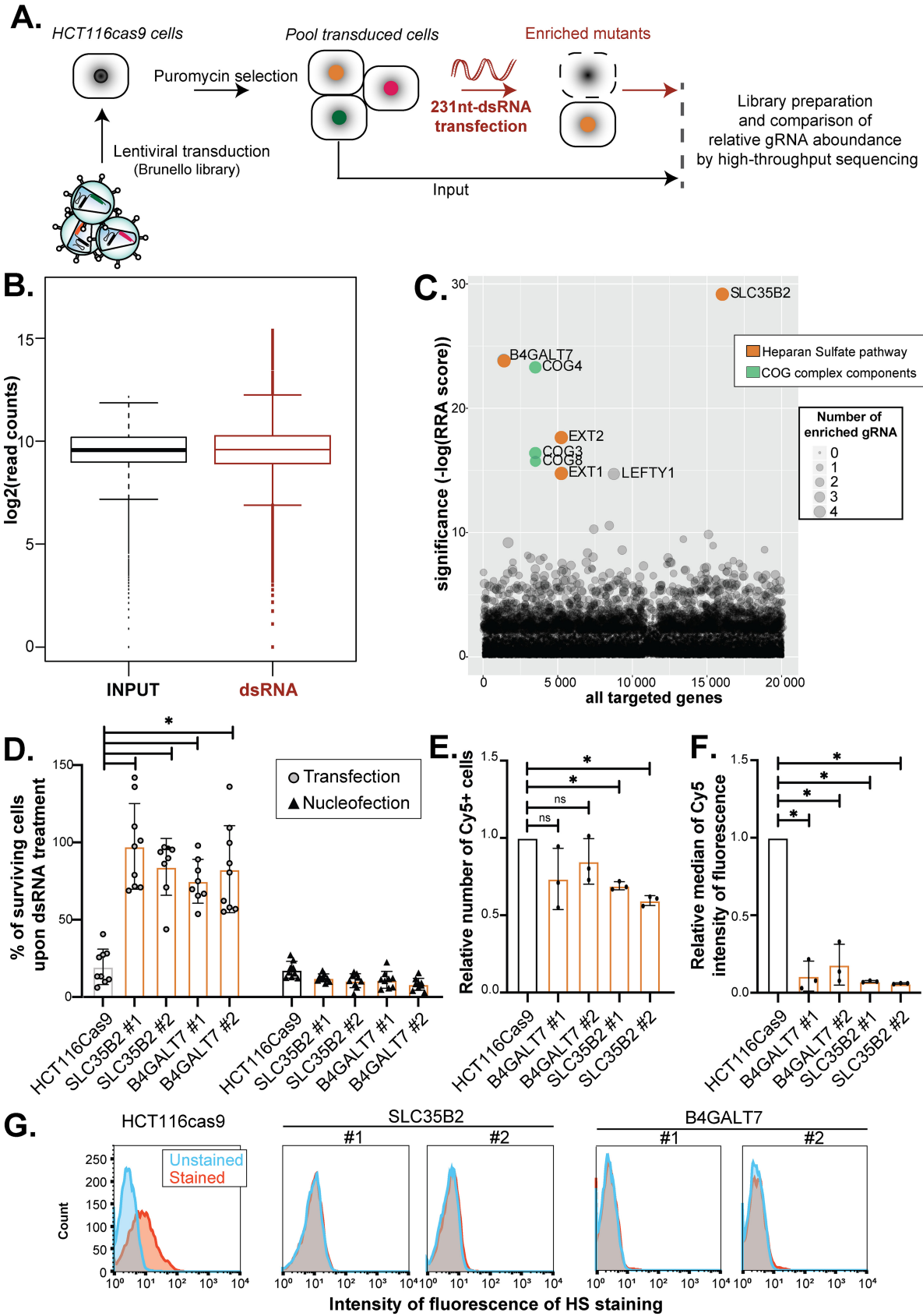


FIG 1 CRISPR-Cas9 survival screen of long dsRNA identifies the extracellular heparan sulfates as necessary for nucleic acid internalization and cell death induction. (A) Schematic representation of the CRISPR-Cas9 approach. *HCT116* cells stably expressing a human codon-optimized
(Continued on next page)

To establish whether impairment of the HS synthesis is directly linked to a defect in dsRNA entry and increased cell survival, we measured the extracellular HS levels in *SLC35B2* and *B4GALT7* KO cells. We measured a substantial reduction of the extracellular HS staining, as assessed by FACS measurement of two independent *SLC35B2* and *B4GALT7* KO clones compared with HCT116 wild-type cells (Fig. 1G). To confirm the importance of HS at the cell surface for liposome-based transfection, we mimicked the HS-defective phenotype by removing extracellular HS in parental HCT116cas9 cells either enzymatically (with heparinase) or chemically (with sodium chlorate [NaClO₃]) (Fig. S3C and D). We tested the transfectability of a GFP-expressing plasmid by measuring either the relative number of GFP-positive cells or the relative median of GFP intensity of fluorescence by FACS analysis. Although the relative number of GFP-positive cells was not significantly reduced by heparinase treatment (Fig. S3C), it caused a reduction in GFP intensity in HCT116cas9-treated cells, thereby recapitulating the GFP plasmid lipofection defect observed in *SLC35B2* and *B4GALT7* KO (Fig. S3D). Moreover, this effect correlated with the reduction of extracellular HS by enzymatic treatment quantified by FACS (Fig. S3E), which demonstrated that extracellular HS are crucial for transfection by lipofection. In the case of NaClO₃ treatment, despite the reduction in both the relative number of GFP-positive cells (Fig. S3C) and the relative median of GFP intensity of fluorescence (Fig. S3D) compared with the control, we could not observe a correlation with a decrease in overall extracellular HS (Fig. S3E). This result could be due to the fact that while a mix of heparinase I and III removes every kind of extracellular heparan sulfates, NaClO₃ impairs only the O-sulfation (21).

Taken together, our results show that knocking out *SLC35B2* and *B4GALT7* results in reduced levels of extracellular HS, which in turn impairs liposome-based transfectability of HCT116 cells. Moreover, the validation of these two top hits indicates that other candidates might be suitable for further analysis and may also have an impact on the dsRNA resistance phenotype.

COG4 is involved in dsRNA-induced cell death partly via the heparan sulfate pathway. Among the significant hits of our genome-wide screen were proteins related to the COG complex, namely, COG4, COG3, and COG8. The COG complex is a heterooctameric complex containing 8 subunits (COG1 to COG8) interacting with numerous proteins mainly involved in intra-Golgi membrane trafficking, such as vesicular coats, Rab proteins, and proteins involved in the SNARE complex (22, 23). This interaction with the trafficking machinery is crucial for the proper functionality of the Golgi apparatus, and mutations in the COG complex result in severe cellular problems, such as glycosylation defects (24–27), which are due to mislocalization of recycling Golgi enzymes (28, 29).

Since we retrieved three out of the eight COG family members in our CRISPR-Cas9 screen suggesting their importance in dsRNA-induced cell death, we tested the effect

FIG 1 Legend (Continued)

S. pyogenes Cas9 protein were transduced with the lentiviral sgRNA library Brunello (MOI, 0.3). Thirty million transduced cells per replicate were selected with 1 μg/ml puromycin to obtain a mutant cell population to cover at least 300× the library. Selective pressure via synthetic long dsRNA (1 μg/ml) was applied to induce cell death (in red). DNA libraries from input cells and cells surviving the dsRNA treatment as three independent biological replicates were sequenced on an Illumina HiSeq 4000 instrument. Comparisons of the relative sgRNA abundance under the input and dsRNA conditions were done using the MAGeCK standard pipeline. (B) Median normalized read count distribution of all sgRNAs for the input (in black) and dsRNA (in red) replicates. (C) Bubble plot of the candidate genes. Significance of robust rank aggregation (RRA) score was calculated for each gene in the dsRNA condition compared with that of input using the MAGeCK software. The number of enriched sgRNAs for each gene is represented by the bubble size. The gene ontology pathways associated with the significant top hits are indicated in orange and green. (D) Viability assay. Cells were transfected (80,000 cells; 1 μg/ml) or nucleofected (200,000 cells; 400 ng) with synthetic long dsRNA, and cell viability was quantified 24 h (nucleofection) or 48 h (transfection) posttreatment using PrestoBlue reagent. The average of at least three independent biological experiments ± SD is shown. One-way ANOVA analysis; *, *P* < 0.05. (E, F) Cy5-labeled dsRNA (80,000 cells; 1 μg/ml) was transfected into HCT116cas9, B4GALT7#1 and 2, and SLC35B2#1 and #2 cells; and Cy5 fluorescence was quantified using FACS (10,000 events). The relative number of the Cy5-positive (Cy5+) cells (E) and the relative median of Cy5 intensity of fluorescence (F) compared to those of HCT116cas9 cells are shown. The average of three independent biological experiments ± SD is shown. Paired *t* test analysis; *, *P* < 0.05. (G) Quantification of extracellular heparan sulfates. FACS analysis of HCT116 control or KO clones stained with the HS-specific antibody 10E4 (in red) compared to unstained samples (in blue) (10,000 events). One representative experiment out of three is shown.

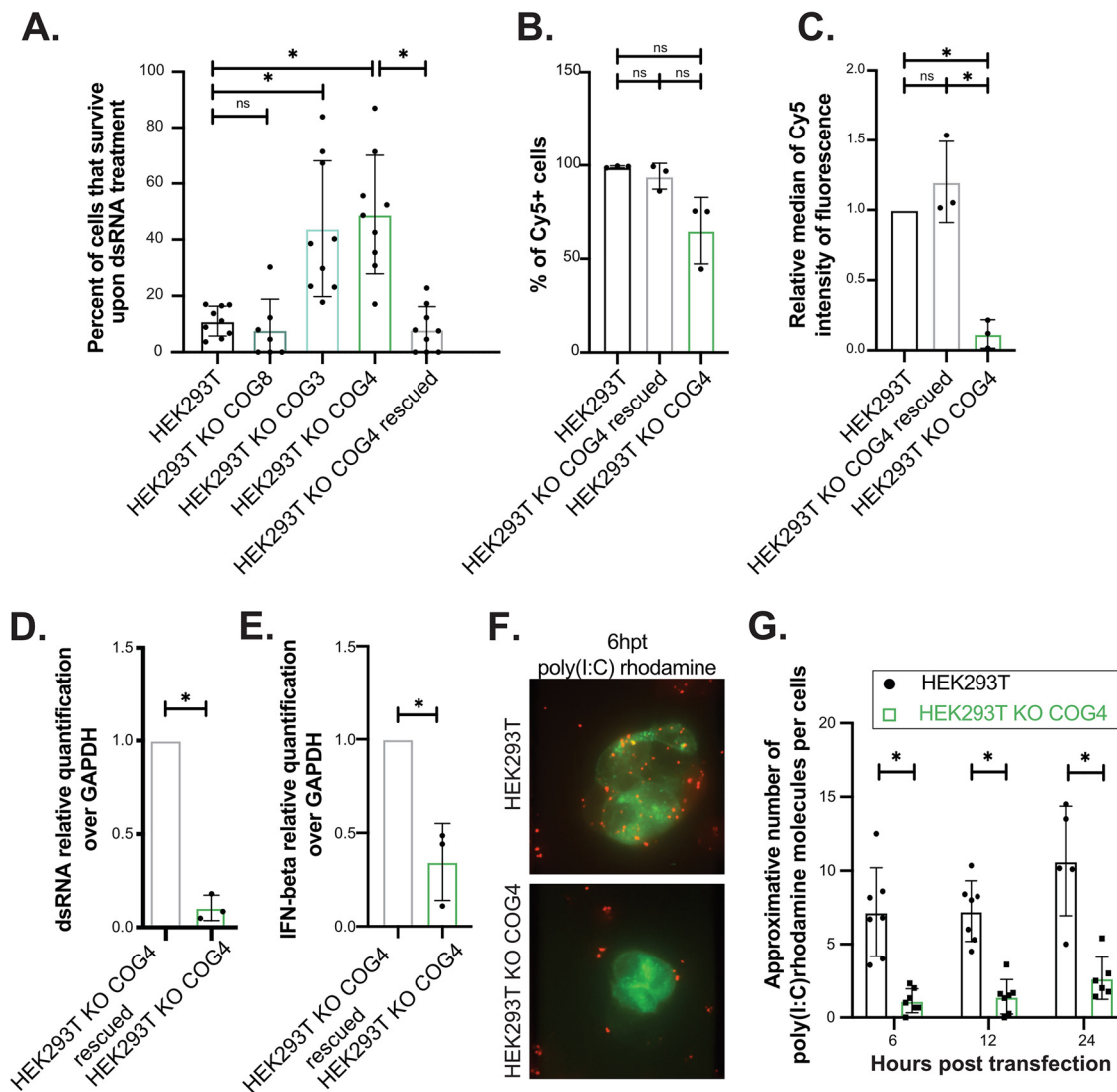


FIG 2 *COG4* is a novel host susceptibility factor to long dsRNA-induced cell death. (A) Viability assay. Cells (80,000 cells; 1 μ g/ml) were transfected with dsRNA, and then the viability of the cells was quantified 48 h posttransfection using PrestoBlue reagent. Data from at least three independent biological experiments are shown. One-way ANOVA analysis; *, $P < 0.05$. (B, C) Cy5-labeled dsRNA transfection (80,000 cells; 1 μ g/ml) in HEK293T, KO *COG4*, and rescued cells. Cy5 fluorescence was quantified using the FACSCalibur platform (10,000 events). The percentage of Cy5+ cells (B) and the relative median of Cy5 intensity of fluorescence (C) compared to parental HEK293T cells are shown. Average of three experiments \pm SD is shown. Paired t test analysis; *, $P < 0.05$. (D, E) qPCR quantification of dsRNA and IFN- β . Cells (300,000 cells; 1 μ g/ml) were transfected with synthetic long dsRNA. Total RNA was extracted 24 h posttransfection and quantified by RT-qPCR. The histogram represents the expression fold change of synthetic dsRNA (D) and IFN- β mRNA (E) relative to GAPDH mRNA in dsRNA-transfected HEK293T KO *COG4* rescued compared to HEK293T KO *COG4*. The average of three independent biological experiments \pm SD is shown. Paired t test analysis; *, $P < 0.05$. (F, G) poly(I:C) rhodamine transfection and immunofluorescence in HEK293T and HEK293T KO *COG4*. Cells were transfected with rhodamine-labeled poly(I:C) (in red) and with a Rab5-GFP plasmid (in green). Images were acquired using a spinning disk microscope at different times posttransfection. Representative pictures (F) and the approximate number of rhodamine-positive foci per cells quantified by counting 7 fields per conditions (G) are shown. Two-way ANOVA analysis; *, $P < 0.05$.

of their inactivation by CRISPR-Cas9. As *COG4* is the most enriched COG gene in our screen, we generated a polyclonal *COG4* KO HCT116cas9 cell line and validated their dsRNA resistance phenotype resulting in an increase survival in response to synthetic dsRNA transfection (see Fig. S4A in the supplemental material). We also observed a reduction in the relative number of Cy5-positives (Cy5+) cells and the median Cy5 fluorescence in *COG4* KO cells relative to the control by FACS analysis (Fig. S4B and C).

To further confirm the involvement of the COG complex, we also tested the effect of dsRNA transfection in previously generated HEK293T KO *COG3*, *COG4*, and *COG8* cells (Fig. 2A) (30). Interestingly, while *COG8* mutants did not display a significant survival

phenotype in response to dsRNA lipofection, *COG3* and *COG4* KO HEK293 cells did. In addition, the survival phenotype could be complemented by stable expression of a *COG4*-GFP construct compared with *COG4* KO cells (Fig. 2A). Moreover, although we could not detect a decrease in the relative number of Cy5-positive (Cy5+) cells in *COG4* KO cells relative to the controls (Fig. 2B), the median Cy5 fluorescence in *COG4* KO cells was significantly reduced compared with both HEK293T and *COG4*-rescued cells (Fig. 2C), thereby indicating a significant decrease in the number of transfected Cy5-labeled RNA molecules per cells.

In agreement, dsRNA accumulation appeared to be significantly reduced, but still present, in HEK293T *COG4* KO cells compared with control cells, as determined by reverse transcriptase quantitative PCR (RT-qPCR) analysis of dsRNA isolated from cells 24 h after transfection (Fig. 2D), and this correlated with reduced IFN- β accumulation in HEK293T KO *COG4* cells compared with control cells (Fig. 2E).

These results indicated that dsRNA transfectability was strongly reduced but not completely impaired in the absence of *COG4* and that dsRNA could be still detected in *COG4* KO cells in order to activate type-I IFN response.

We confirmed the reduced internalization of dsRNA in *COG4* mutant cells by transfecting rhodamine-labeled poly(I-C), a synthetic dsRNA analog, in HEK293T *COG4* KO or WT cells (Fig. 2F) and by counting the number of poly(I-C) foci per cell at 6, 12, and 24 h posttransfection (Fig. 2G). We could observe a significant reduction in rhodamine-positive foci in HEK293T *COG4* KO during the time course, suggesting a defect in dsRNA internalization, which could explain the increased survival phenotype.

In order to assess whether the *COG4* KO survival phenotype was associated with a defect in the heparan sulfate pathway, we stained extracellular HS and measured the HS expression by FACS analysis. We observed a decrease of extracellular HS in KO *COG4* cells compared with control cells (WT and rescued), which demonstrated that the COG complex is related to the HS biosynthesis pathway (Fig. S4D).

The reduction in extracellular HS could correlate with a decrease in transfectability and explain the survival phenotype in KO *COG4* cells. Surprisingly, however, lipofection of a GFP-expressing plasmid indicated that HEK293T *COG4* KO cells are still transfectable with a plasmid DNA compared with control cells, as observed by FACS analysis (Fig. S4E and F).

Altogether, these findings indicate that the COG complex is involved in HS biosynthesis and that removal of *COG4* results in a lower accumulation of HS at the cell surface, which most likely translates to a reduced transfectability of dsRNA. However, as opposed to the observations in *SLC35B2* or *B4GALT7* KO cells, the cells are still transfectable with a plasmid DNA and, although to a lower extent, with dsRNA. Interestingly, the increased cell survival phenotype of *COG4* KO cells upon dsRNA transfection does correlate with a reduced, but still measurable, IFN- β production.

Cell survival-based genome-wide CRISPR-Cas9 screen identifies *COG4* as a permissivity factor to SINV. SINV is a small enveloped virus with a single-stranded RNA genome of positive polarity. The virus belongs to the *Togaviridae* family, *Alphavirus* genus, and is considered the model for other medically important viruses, such as chikungunya virus (CHIKV) and Semliki Forest virus (SFV). During its infectious cycle, SINV produces dsRNA as a replication intermediate and induces cytopathic effects in mammalian cells, leading to cell death within 24 to 48 h postinfection (31).

In order to identify host genes that are related to SINV-induced cell death and infection, we performed a CRISPR-Cas9 knockout screen in HCT116cas9 cells, which are susceptible to this virus (Fig. 3A and Fig. S1). After transduction with the CRISPR lentiviral genome-wide knockout library, puromycin-resistant HCT116 cells were infected with SINV-GFP at a multiplicity of infection (MOI) of 0.1 and selected for cell survival. Using the MAGeCK software (16), we assessed the normalized read count distribution of the control and SINV-infected biological triplicates, which, despite a quite homogenous sgRNA distribution, showed the presence of few outliers upon selection (Fig. 3B). We identified two genes that were significantly enriched with a false

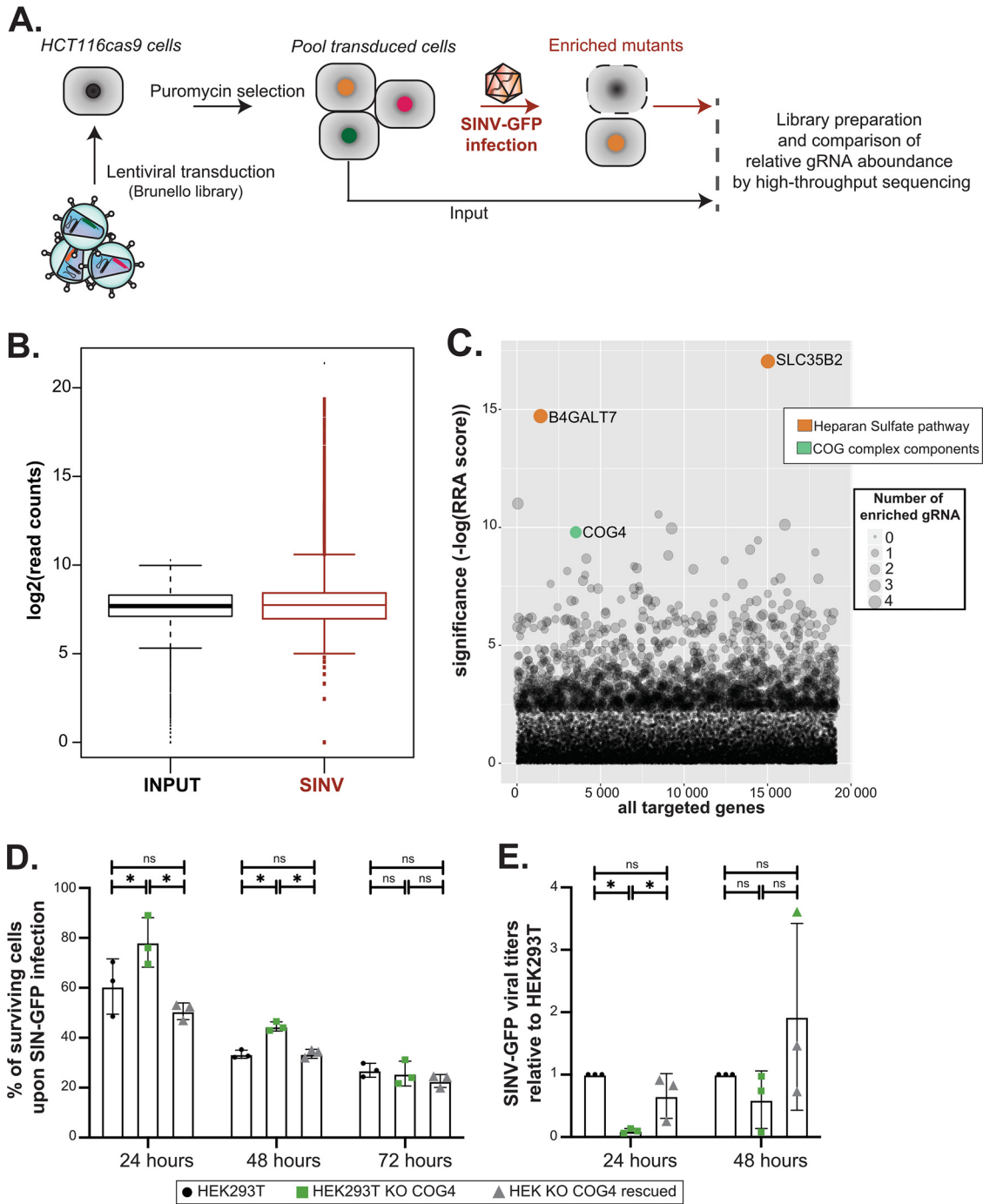


FIG 3 CRISPR-Cas9 screen identifies *COG4* as a permissivity factor to SINV. (A) Schematic representation of the CRISPR-Cas9 approach. HCT116 cells stably expressing a human codon-optimized *S. pyogenes* Cas9 protein were transduced with the lentiviral sgRNA library Brunello (MOI, 0.3). Thirty million transduced cells per replicate were selected with 1 $\mu\text{g}/\text{ml}$ puromycin to obtain a mutant cell population to cover at least 300 \times the library. Selective pressure via SINV infection (MOI, 0.1) was applied to induce cell death (in red). DNA libraries from input cells and cells surviving the dsRNA treatment as three independent biological replicates were sequenced on an Illumina HiSeq 4000 instrument. Comparisons of the relative sgRNA abundance under the input and dsRNA conditions were done using the MAGeCK standard pipeline. (B) Median normalized read count distribution of all sgRNAs for the input (in black) and SINV (in red) replicates. (C) Bubble plot of the candidate genes. Significance of RRA score was calculated for each gene under the dsRNA condition compared with that of input using the MAGeCK software. The number of enriched sgRNAs for each gene is represented by the bubble size. The gene ontology pathways associated with the significant top hits are indicated in orange and green. (D) Viability of cells upon SINV infection. Cells were infected with SINV at MOI of 0.1, and then the viability of the cells was quantified 24, 48, and 72 h postinfection using PrestoBlue reagent. One-way ANOVA analysis; *, $P < 0.05$. (E) SINV GFP plaque assay. WT, COG4KO, and rescued HEK293T cells were infected with SINV GFP for 24 and 48 h at an MOI of 1, and the supernatant was collected in order to measure viral production. The fold change in titer relative to HEK293T arbitrarily set to 1 is shown. The average of three independent biological experiments \pm SD is shown. Paired *t* test analysis; *, $P < 0.05$.

discovery rate lower than 25% (FDR25%), notably *SLC35B2* and *B4GALT7* (see Data Set S3 in the supplemental material, Fig. 3C). Genes of the heparan sulfate pathway have been previously found in genome-wide CRISPR-Cas9 loss-of-function studies looking for factors involved in the accumulation of viruses, such as influenza, Zika, and chikungunya viruses (11, 32, 33). Interestingly, among the top-ranking hits, we retrieved *COG4*, which was not previously associated with SINV infection (Fig. 3C).

To validate the involvement of *COG4* during SINV infection, we infected HEK293T, *COG4* KO, or *COG4* KO-rescued HEK293T cells with SINV and measured cell viability at 24, 48, and 72 hpi. The cell viability assay revealed that the *COG4* KO cells were less sensitive at early time points of SINV infection (24 and 48 hpi), but this tendency disappeared at 72 hpi (Fig. 3D). In agreement, the determination of viral titer by plaque assay showed that *COG4* KO HEK293T cells produced significantly fewer infectious viral particles than HEK293T or *COG4*-rescued cells at 24 hpi but not at 48 hpi, underlining a possible delay in the infection and virus-induced cell death (Fig. 3E). We also observed that GFP accumulated to lower levels in *COG4* KO than in WT cells both at 24 and 48 h postinfection (hpi) (Fig. S5A). Finally, we noticed that the reduced viral production in *COG4* KO cells was associated with a reduced accumulation of viral dsRNA in the cytoplasm when we infected WT or *COG4* KO cells with SINV-GFP and performed immunostaining with the anti-dsRNA J2 antibody 24 hpi (Fig. S5B). Overall, our results indicate that *COG4* expression is needed for an efficient SINV infection and that its absence can delay the infection, thereby increasing cell survival in *COG4* KO cells.

DISCUSSION

Several CRISPR-Cas9 screens aimed at identifying factors required for infection by specific viruses have been described in the literature, but to our knowledge, none has been designed to look at the effect of the only common factor between all those viruses, i.e., dsRNA. Here, we used the Brunello sgRNA lentiviral library to screen for genes involved in HCT116 cell survival to synthetic dsRNA transfection and to SINV infection. This screen allowed us to identify components of the heparan sulfate biosynthesis pathway and of the COG complex that are critical host factors in the cellular response to both long dsRNA transfection and SINV infection challenges. It has been reported that cell survival-based CRISPR screens for viral host factors are biased toward genes linked to the initial steps of the infection and even more so to viral entry (11, 34). Thus, in our case, HS is a well-known factor required for SINV entry due to virus adaptation to cell culture (35). We also retrieved genes of the HS pathway in our dsRNA-based screen, and we confirmed the importance of extracellular HS for dsRNA-induced toxicity. This is mostly due to a decrease of cell transfectability when HSs are missing, which is linked to the fact that the polyplexes used for transfection are positively charged and can interact electrostatically with glycosaminoglycans (36, 37). Our work also addresses limitations of survival-based CRISPR-Cas9 screens. Thus, in this study, the selection pressure was too strong to allow the identification of genes intervening after the entry step, thereby making the screen less sensitive. Adjusting the selection procedure by reducing the concentration of dsRNA or increasing the duration of treatment may allow the identification of hits not solely implicated in the transfection process but also the innate response of the cells to either dsRNA or the transfection agent. Alternatively, new strategies should be designed to overcome this problem, such as using fluorescent-based cell sorting in order to be less stringent in the selection.

In addition to the HS pathway, we identified members of the COG complex, and more specifically *COG4*, as factors involved in dsRNA transfection and SINV infection. Loss-of-function *COG4* mutant cells show a dsRNA-resistant phenotype as well as a reduction in extracellular HS expression, which is similar to previously published reports for other COG proteins (33, 38). Surprisingly, even if the removal of *COG4* expression results in a defect in the HS pathway, we were still able to transfect the KO *COG4* cell line either with a plasmid encoding GFP or, although to a lesser extent, dsRNA. In addition, the dsRNA molecules that are able to enter into *COG4* KO HEK293T cells are still sufficient to induce the IFN- β mRNA production, indicating that the innate immune

response is still functional in these mutant background. Nonetheless, cell death induced by dsRNA appears to be lower in *COG4* KO cells, most likely due to a delay in the infection.

Future work will be needed to assess whether this phenotype upon SINV infection is correlated only with a defect in HS biogenesis in *COG4* mutants or with other functions of *COG4*. The increased cell survival to synthetic dsRNA transfection and viral infection of *COG4* KO cells compared to WT cells opens several interesting perspectives. Indeed, since the COG complex is related to glycosylation and membrane trafficking (23, 25, 39, 40), deficiency in one or more of its components could potentially lead to a glycosylation and/or subcellular localization defect of components of the innate immune response or of the apoptosis pathway, although this possibility remains to be formally proven. The difference of transfectability of plasmid DNA and dsRNA in *COG4* KO cells is also intriguing and could indicate that different kinds of nucleic acids do not necessarily use the exact same routes to enter the cells upon liposome-based transfection. Finally, there could be other defects linked to COG deficiencies (39, 41) that could account for our observations, and elucidating those defects will require further work. It is particularly interesting that *COG3* and *COG4* knockout cells display a dsRNA-induced cell death resistance phenotype, while *COG8* mutants do not. This finding implies that only part of the COG complex is involved in dsRNA uptake.

In conclusion, our work uncovered *COG4* as a new player in HS production, which is required for both SINV infection and dsRNA transfection. These results also highlight that synthetic dsRNA is a powerful tool for identifying novel key pathways of the cellular response to RNA viruses.

MATERIALS AND METHODS

Cell culture and virus. HCT116, HEK293T, HEK293T *COG* KOs, BHK-21, and Vero R cells were maintained in Dulbecco's modified Eagle medium (DMEM) and 4.5 g/liter glucose (Gibco, Thermo Fisher Scientific Inc.) supplemented with 10% fetal bovine serum (FBS) (TaKaRa) in a humidified atmosphere of 5% CO₂ at 37°C. HEK293T *COG3*, *COG8*, and *COG4* KO and *COG4* KO stably rescued with *COG4*-GFP were described previously (42, 43). HCT116cas9 and HEK293T *COG4* rescued were maintained in the same medium with an addition of 10 μg/ml blasticidin. HCT116 KO clones (*COG4*, *SLC35B2*#1, *SLC35B2*#2, *B4GALT7*#1, and *B4GALT7*#2) were maintained in the same medium with an addition of 10 μg/ml blasticidin and 1 μg/ml puromycin.

SINV wild type (SINV WT) or SINV expressing the green fluorescent protein (SINV GFP) were produced as previously described (44) in BHK-21 cells. In SINV GFP, the promoter of SINV subgenomic RNA was duplicated and inserted at the 3' extremity of the viral genome, and the GFP sequence was then inserted after this new promoter. Cells were infected with either SINV WT or SINV GFP at an MOI of 10⁻¹, and samples were harvested at 24 or 48 hours postinfection (hpi).

Standard plaque assay. Ten-fold dilutions of the viral supernatant were prepared. Fifty-microliter aliquots were inoculated onto Vero R cell monolayers in 96-well plates for 1 hour. Afterward, the inoculum was removed, and cells were cultured in 2.5% carboxymethyl cellulose for 72 h at 37°C in a humidified atmosphere of 5% CO₂. Plaques were counted manually under the microscope. For plaque visualization, the medium was removed and cells were fixed with 4% formaldehyde for 20 min and stained with 1× crystal violet solution (2% crystal violet [Sigma-Aldrich], 20% ethanol, and 4% formaldehyde).

J2 immunostaining. HEK293T or KO *COG4* HEK293T cells were plated onto a Millipore EZ slide (Millipore) and were infected with SINV at an MOI of 0.1 for 24 h. Cells were fixed with 4% formaldehyde diluted in 1× phosphate-buffered saline (PBS) for 10 min at room temperature (RT), followed by incubation in blocking buffer (0.2% Tween X-100, 1× PBS, and 5% normal goat serum) for 1 h. J2 antibody (Scicons) diluted in blocking buffer at 1:1,000 was incubated overnight at 4°C. Between each step, cells were washed with 1× PBS-0.2% Tween. Secondary antibody goat anti-mouse Alexa 594 (ThermoFisher) diluted at 1:1,000 in 1× PBS-0.2% Tween was incubated for 1 h at room temperature. After 4',6'-diamidino-2-phenylindole (DAPI) staining (1:5,000 dilution in 1× PBS for 5 min), slides were mounted with a coverslip over antifading medium and observed by epifluorescence microscopy using the BX51 (Olympus) microscope with a 40× lens objective.

Generation of HCT116cas9 line. The HCT116cas9 cells, expressing the human codon-optimized *Streptococcus pyogenes* Cas9 protein, were obtained by transducing the wild-type HCT116 colorectal carcinoma cell line (ATCC CCL-247) with a lentiCas9-BLAST lentiviral vector (no. 52962; Addgene). Briefly, wild-type HCT116 cells were cultured in standard DMEM (Gibco) medium supplemented with 10% fetal bovine serum (FBS; Gibco) and 100 U/ml of penicillin-streptomycin (Gibco) at 37°C in 5% CO₂. The cells were transduced at 80% confluence in a 10-cm tissue culture plate, using 6 ml of lentiviral supernatant supplemented with 4 μg/ml of Polybrene (H9268; Sigma) for 6 hours. The transduction medium was replaced with fresh growing medium for 24 h before starting the selection. Transduced HCT116cas9 cells

were selected for 10 days and maintained in growing medium supplemented with 10 $\mu\text{l/ml}$ of blasticidin (Invivogen).

High-titer lentiviral sgRNA library production. The production of a high-titer human sgRNA Brunello lentiviral library, which contains 4 sgRNAs per gene (15) (no. 73178; Addgene), was performed by transfecting HEK293T cells in five 15-cm tissue culture plates using the polyethyleneimine (PEI) (linear; molecular weight [MW], 25,000; no. 23966-1-A; Polysciences) transfection method (45). Briefly, for each 15-cm plate containing 20 ml of medium, 10 μg of sgRNA library, 8 μg of psPAX2 (plasmid no. 12260; Addgene), and 2 μg of pVSV-G (plasmid no. 138479) diluted in 500 μl of 150 mM NaCl were combined with 40 μl of PEI (1.25 mg/ml) dissolved in 500 μl of 150 mM NaCl. The mix was incubated for 30 minutes at room temperature, and the formed complexes were added dropwise on the cells. After 6 hours, the medium was replaced, and the viral supernatant was collected after 48 hours and after 72 hours. The supernatant was filtered through a 0.45- μm polyethersulfone (PES) filter and the viral particles concentrated 100 times using the Lenti-X concentrator (TaKaRa) before storage at -80°C . The viral titer was established by counting puromycin-resistant colonies formed after transducing HCT116 cells with serial dilutions of the viral stock. HCT116cas9 cells were transduced with lentivirus-packaged Brunello sgRNA library at an MOI of 0.3. The lentiviral library has been sequenced to verify that all the lenti-sgRNA are represented.

Genome-wide CRISPR-Cas9 knockout screens. For each replicate ($n = 3$), 5 million stably transduced cells/dish were seeded in six 15 cm^2 plates in order to keep a 300 \times representativity of the sgRNA library. Untreated samples (input) were collected as controls. One day later, cells were either lipofected with 1 $\mu\text{g/ml}$ dsRNA-citrine or infected with SINV at MOI of 0.1 and cultured at 37°C and 5% CO_2 . Cells were washed with $1 \times$ PBS 48 hours posttreatment, to remove dead cells, and fresh medium was added to surviving clones. Cells were expanded, and all cells were collected 6 days post-dsRNA transfection and 18 days post-SINV infection.

Genomic DNA was isolated by resuspending the cell pellet in 5 ml of resuspension buffer (50 mM Tris-HCl [pH 8.0], 10 mM EDTA, and 100 $\mu\text{g/ml}$ RNaseA), and 0.25 ml of 10% SDS was added and incubated 10 min at RT after mixing. After incubation, the sample was sonicated and incubated 30 min at RT with 10 μl of proteinase K (10 mg/ml). A total of 5 ml of a phenol/chloroform/isoamyl alcohol solution was added, followed by a centrifuge step for 60 min at $12,000 \times g$ and 20°C . The upper phase was transferred into a new tube, and 500 μl of 3M NaAc and 5 ml of isopropanol was added and incubated overnight at RT, followed by a centrifuge step for 30 min at 20°C and $12,000 \times g$. The pellet was washed using EtOH and dissolved in H_2O .

Illumina P5- and P7-barcoded adaptors were added by PCR on genomic DNA (gDNA) samples according to the GoTaq protocol (Promega). PCR amplicons were gel purified and sequenced on a HiSeq 4000 instrument (Illumina) to obtain about 30 million reads for each sample. The enrichment of sgRNAs was analyzed using MaGeCK with default parameters (16). The primers used to generate the PCR products are listed in Table S1 in the supplemental material. The results of the dsRNA and SINV screen are available in Data Set S1 and S2, respectively

Generation of monoclonal SLC35B2 and B4GALT7 and polyclonal COG4 knockout HCT116 cell lines. The sgRNA expression vectors targeting SLC35B2, B4GALT7, or COG4 (sgRNA sequences selected were the 2 most enriched sgRNA from the Brunello library in the dsRNA screen) genes were produced by annealing the “sense” and “antisense” oligonucleotides (Table S1) at a concentration of 10 μM in 10 mM Tris-HCl (pH 8.0) and 50 mM MgCl_2 in 100 μl . The mixture was incubated at 95°C for 5 minutes and then allowed to cool down to room temperature. The oligonucleotide duplex thus formed was cloned into the BbsI restriction site of the plasmid pKLV-U6gRNA (BbsI)-pGKpuro2ABFP (no. 62348; Addgene). The lentiviral supernatant from the single transfer vector was produced by transfecting HEK293T cells (ATCC CRL-3216) with the transfer vector psPAX2 packaging plasmid (no. 12260; Addgene) and the pVSV envelope plasmid (no. 8454; Addgene) in the proportion 5:4:1 using Lipofectamine 2000 (ThermoFisher) reagent according to manufacturer’s protocol. Standard DMEM (Gibco) supplemented with 10% fetal bovine serum (FBS; Gibco) and 100 U/ml of penicillin-streptomycin (Gibco) was used for growing HEK293T cells and for lentivirus production. One 10-cm plate of HEK293T cells at 70% to 80% confluence was used for the transfection. The medium was replaced 8 hours posttransfection. After 48 h, the medium containing viral particles was collected and filtered through a 0.45- μm PES filter. The supernatant was directly used for transfection or stored at -80°C . A 6-well plate of HCT116cas9 cells at 80% confluence was transduced using 600 μl of the lentiviral supernatant (300 μl of each lentivirus produced for each duplex) supplemented with 4 $\mu\text{g/ml}$ Polybrene (Sigma) for 6 h. The transduction medium was then changed with fresh DMEM for 24 hours, and then the transduced cells were selected using DMEM containing 10 $\mu\text{g/ml}$ blasticidin (Invivogen) and 1 $\mu\text{g/ml}$ puromycin (Invivogen). Genomic DNA was isolated from individual colonies, and KO clones were screened by PCR (primers in Table S1). The expected WT band for SLC35B2 is 469 bp and the mutant band is 132 bp. For B4GALT7, the WT band is 341 bp and mutant band is 180 bp. For laboratory purposes, the SLC35B2 clones have been generated into HCT116cas9 cells that are expressing mCherry and citrine due to integration of miReporter-PGK (no. 82477; Addgene).

Nucleic acid delivery. Transfection using Lipofectamine 2000 (no. 11668019; Invitrogen) was performed following the manufacturer’s instructions. For nucleofection, cells were nucleofected using Nucleofector SE solution and reagent into a Nucleocuvette following the manufacturer’s instructions using the 4D-Nucleofector system (Lonza). The cell number and nucleic acid amounts are indicated in each figure legend. P-EGFP-N1 (plasmid no. 2491; Addgene) was used in transfection and nucleofection experiments as a control.

Viability assay. PrestoBlue (PB) reagent (no. A13261; ThermoFisher) was used for the viability assay according to the manufacturer's protocol. After 24 to 48 hours posttreatment (SINV, dsRNA transfection/nucleofection), cells were incubated with PB reagent, and cell viability was assessed by measuring the fluorescence (excitation, 570 nm; emission, 590 nm) after a 20-min incubation using a SAFAS spectrofluorometer (Xenius XC). Cell viability was expressed as a percent relative to untreated cells.

Heparinase and sodium chlorate treatment and heparan sulfate staining. One million cells were treated with 2 U of a heparinase I and III blend from *Flavobacterium heparinum* (no. H3917; Merck) for 1 h at 37°C and 5% CO₂ in DMEM, and then cells were reverse transfected with 2 μg of GFP using Lipofectamine 2000 (Invitrogen) in 6-well plate.

HCT116cas9 cells were grown in 50 mM sodium chlorate (no. 1.06420; Merck), DMEM, and 10% FBS for at least 48 h, and then 150,000 cells were reverse transfected with 500 ng of GFP using Lipofectamine 2000 (Invitrogen) in a 24-well plate.

At 24 (heparinase) or 48 (sodium chlorate) hours posttreatment, cells were detached using PBS and 0.02% EDTA, and then heparan sulfate was stained using 1:30 of F58-10E4 as the primary antibody (catalog no. 370255-S; Amsbio) in PBS and 3% bovine serum albumin (BSA) for 30 to 40 minutes on ice. Next, cells were washed with PBS and 1% FBS, incubated with 1:30 anti-mouse Alexa Fluor 594 (A-11032; Thermo) in PBS and 3% BSA, washed twice using PBS and 1% FBS, and then analyzed on a FACSCalibur flow cytometer.

dsRNA preparation. PCR fragments corresponding to 231 nucleotides (nt) of the citrine coding sequence were amplified from the ES-FUCCI plasmid (plasmid no. 62451; Addgene) using primers containing the T7 promoter sequence with 2 distinct PCR fragments for the positive-sense or negative-sense RNA. Primers used to generate the PCR products are listed in Table S1. The PCR fragments were produced using the DyNAzyme EXT DNA polymerase (F-505S; Thermo Scientific) and purified using Monarch DNA extraction (T1020L; New England Biolabs). *In vitro* transcription (IVT) with a homemade T7 RNA polymerase was performed for 4 hours at 37°C. To label the IVT RNA, 1/10th of Cy5-CTP (Amersham CyDye Fluorescent Nucleotides Cy5-CTP; GE Healthcare Life Sciences) was included in the IVT reaction. IVT RNA was digested with DNase I (EN0525; Thermo Scientific) for 30 min at 37°C, the IVT product was purified, and the unincorporated nucleotides were removed and size checked using UV shadow (8% acrylamide-urea gel), followed by phenol-chloroform extraction and nanodrop quantification for each strand. We then mixed an equal quantity of positive-strand and negative-strand RNA and heated the mixture for 5 minutes at 95°C, followed by slow cool down to RT. The integrity of the dsRNA was then checked by RNases T1 (EN0541; Thermo Scientific) and V1 (AM2275; Ambion) digestion.

Microscopy. Imaging of cells treated with the dsRNA/GFP plasmid was carried out on the Observer A1 (Zeiss) microscope and analyzed using Fiji (46). Images of cells transfected with poly(I:C) (LMW) rhodamine (tlrl-piwr; Invivogen) (1.8 μg/ml, 24 h postplating of 76,000 cells) into Lab-Tek chambered coverglass (155411; Thermo Scientific) were acquired using a 100× Plan Apochromat oil immersion NA1.4 objective on a spinning disk system, Axio Observer Z1 (Zeiss), every 20 minutes for 72 hours. All pictures were acquired under the same conditions (laser power and amplification gain) and then processed with Fiji. Images of cells infected with SINV stained with J2 antibody were carried out on a BX51 microscope (Olympus).

FACS analysis. The cells intended for analysis by flow cytometry were recovered mechanically (PBS and 0.5 mM EDTA) or using trypsin, washed in PBS, and then suspended in PBS and 1% FBS. Each acquisition included at least 10,000 events and was performed on the FACSCalibur (BD Bioscience) device. The data produced were processed using FlowJo software.

RT-qPCR analysis. Total RNA was isolated using TRIzol (15596026; Invitrogen) following the manufacturer's instructions. A total of 1 μg of RNA was reverse transcribed using SuperScript IV Vilo master mix (11756050; Invitrogen) according to the manufacturer's instructions. Real-time PCR was performed using SYBR green (4309155; Applied Biosystems) and primers listed in Table S1 at an annealing temperature of 60°C on a CFX96 thermal cycler (Bio-Rad). Generated data were analyzed using the CFX Manager software (Bio-Rad).

Western blot analysis. Proteins were extracted using radioimmunoprecipitation assay (RIPA) lysis buffer. Proteins were quantified by the Bradford method, and 20 to 30 μg of total protein extract was loaded on 4% to 20% Mini-Protean TGX precast gels (Bio-Rad). After transfer onto a nitrocellulose membrane, equal loading was verified by Ponceau staining. Membranes were blocked in 5% milk and probed with the following antibodies: anti-Flag M2 (F1804; Sigma) and anti-GAPDH (clone 6C5, MCA4739P; Bio-Rad). Detection was performed using a chemiluminescent substrate (ThermoFisher).

Data availability. The CRISPR-Cas9 screen sequencing data discussed in the manuscript have been deposited on NCBI Sequence Read Archive (SRA) and have been attributed the BioProject identifier (ID) PRJNA662202. It can be accessed at the following URL: <https://submit.ncbi.nlm.nih.gov/subs/bioproject/SUB8109948/overview>.

SUPPLEMENTAL MATERIAL

Supplemental material is available online only.

FIG S1, TIF file, 1.8 MB.

FIG S2, TIF file, 2.4 MB.

FIG S3, TIF file, 2.5 MB.

FIG S4, TIF file, 0.5 MB.

FIG S5, TIF file, 2.2 MB.

TABLE S1, PDF file, 0.01 MB.

DATA SET S1, TXT file, 4.7 MB.

DATA SET S2, TXT file, 1.5 MB.

DATA SET S3, TXT file, 1.6 MB.

ACKNOWLEDGMENTS

We thank members of the Pfeffer laboratory for discussion, Delphine Richer for technical help, Jean-Daniel Fauny for help with the spinning disk microscope, Frédéric Gros for help with FACS analysis, and Carla Saleh for providing us the SINV WT and GFP clones.

This work was funded by the European Research Council (ERC-CoG-647455 RegulRNA) and was performed under the framework of the LABEX ANR-10-LABX-0036_NETRINA and of ANR-17-EURE-0023, which benefits from funding from the state managed by the French National Research Agency as part of the Investments for the Future program. This work has also received funding from the People Program (Marie Curie Actions) of the European Union's Seventh Framework Program (FP7/2007-2013) under REA grant agreement no. PCOFUND-GA-2013-609102, through the PRESTIGE program coordinated by Campus France (to E.G.), and from the French Minister for Higher Education, Research and Innovation (PhD contract to O.P.). V.L. was supported by the National Institutes of Health (R01GM083144).

Sequencing was performed by the GenomEast platform, a member of the "France Génomique" consortium (ANR-10-INBS-0009).

S.P. and E.G. conceived the project. S.P., E.G., and O.P. designed the work and analyzed the results. O.P., E.G., and R.P.N. performed the experiments. E.G. and O.P. set up the CRISPR-Cas9 screens, and R.P.N. generated the lentivirus library and the HCT16-Cas9 cell line. O.P. and R.P.N. performed the bioinformatics analysis of the screens. O.P. generated the SLC35B2 and B4GALT7 KO clones. O.P. generated IVT dsRNA and perform validation of cell survival. E.G. produced the SINV GFP viral stock, performed the infections, and analyzed viral titers. O.P. performed FACS analyses. E.G. and O.P. performed the immunofluorescence assays. O.P. analyzed the live-imaging microscopy data. V.L. provided the COG KO cells and antibodies. O.P., E.G., and S.P. wrote the manuscript with input from the other authors. S.P. and E.G. coordinated the work. S.P. ensured funding. All authors reviewed the final manuscript.

REFERENCES

- Bomsel M, Alfsen A. 2003. Entry of viruses through the epithelial barrier: pathogenic trickery. *Nat Rev Mol Cell Biol* 4:57–68. <https://doi.org/10.1038/nrm1005>.
- Rusnati M, Vicenzi E, Donalizio M, Oreste P, Landolfo S, Lembo D. 2009. Sulfated K5 Escherichia coli polysaccharide derivatives: a novel class of candidate antiviral microbicides. *Pharmacol Ther* 123:310–322. <https://doi.org/10.1016/j.pharmthera.2009.05.001>.
- Byrnes AP, Griffin DE. 1998. Binding of Sindbis virus to cell surface heparan sulfate. *J Virol* 72:7349–7356. <https://doi.org/10.1128/JVI.72.9.7349-7356.1998>.
- Smith TJ, Cheng RH, Olson NH, Peterson P, Chase E, Kuhn RJ, Baker TS. 1995. Putative receptor binding sites on alphaviruses as visualized by cryoelectron microscopy. *Proc Natl Acad Sci U S A* 92:10648–10652. <https://doi.org/10.1073/pnas.92.23.10648>.
- Wahlberg JM, Bron R, Wilschut J, Garoff H. 1992. Membrane fusion of Semliki Forest virus involves homotrimers of the fusion protein. *J Virol* 66:7309–7318. <https://doi.org/10.1128/JVI.66.12.7309-7318.1992>.
- Weber F, Wagner V, Rasmussen SB, Hartmann R, Paludan SR. 2006. Double-stranded RNA is produced by positive-strand RNA viruses and DNA viruses but not in detectable amounts by negative-strand RNA viruses. *J Virol* 80:5059–5064. <https://doi.org/10.1128/JVI.80.10.5059-5064.2006>.
- Schlee M, Hartmann G. 2016. Discriminating self from non-self in nucleic acid sensing. *Nat Rev Immunol* 16:566–580. <https://doi.org/10.1038/nri.2016.78>.
- Stetson DB, Medzhitov R. 2006. Type I interferons in host defense. *Immunity* 25:373–381. <https://doi.org/10.1016/j.immuni.2006.08.007>.
- García MA, Meurs EF, Esteban M. 2007. The dsRNA protein kinase PKR: virus and cell control. *Biochimie* 89:799–811. <https://doi.org/10.1016/j.biochi.2007.03.001>.
- Shalem O, Sanjana NE, Zhang F. 2015. High-throughput functional genomics using CRISPR-Cas9. *Nat Rev Genet* 16:299–311. <https://doi.org/10.1038/nrg3899>.
- Han J, Perez JT, Chen C, Li Y, Benitez A, Kandasamy M, Lee Y, Andrade J, tenOever B, Manicassamy B. 2018. Genome-wide CRISPR/Cas9 screen identifies host factors essential for influenza virus replication. *Cell Rep* 23:596–607. <https://doi.org/10.1016/j.celrep.2018.03.045>.
- Park RJ, Wang T, Koundakjian D, Hultquist JF, Lamothe-Molina P, Monel B, Schumann K, Yu H, Krupczak KM, Garcia-Beltran W, Piechocka-Trocha A, Krogan NJ, Marson A, Sabatini DM, Lander ES, Hacohen N, Walker BD. 2017. A genome-wide CRISPR screen identifies a restricted set of HIV host dependency factors. *Nat Genet* 49:193–203. <https://doi.org/10.1038/ng.3741>.
- Zhang R, Miner JJ, Gorman MJ, Rausch K, Ramage H, White JP, Zuiani A, Zhang P, Fernandez E, Zhang Q, Dowd KA, Pierson TC, Cherry S, Diamond MS. 2016. A CRISPR screen defines a signal peptide processing pathway required by flaviviruses. *Nature* 535:164–168. <https://doi.org/10.1038/nature18625>.
- Golden RJ, Chen B, Li T, Braun J, Manjunath H, Chen X, Wu J, Schmid V, Chang T-C, Kopp F, Ramirez-Martinez A, Tagliabracchi VS, Chen ZJ, Xie Y, Mendell JT. 2017. An Argonaute phosphorylation cycle promotes microRNA-mediated silencing. *Nature* 542:197–202. <https://doi.org/10.1038/nature21025>.

